Improving Computer Interaction for Users with Visual Acuity Deficiencies through Inverse Point Spread Function Processing

Miguel Alonso Jr.
Department of Electrical and Computer Engineering
Florida International University
malons05@fiu.edu

Armando Barreto
Department of Electrical and Computer Engineering
Florida International University
barretoa@fiu.edu

Julie A. Jacko
School of Industrial & Systems Engineering
Georgia Institute of Technology
julie.jacko@isye.gatech.edu

Malek Adjouadi
Department of Electrical and Computer Engineering
Florida International University
adjouadi@fiu.edu

Maroof Choudhury
Department of Biomedical Engineering
Florida International University
mchou001@fiu.edu

Abstract

Human beings take advantage of their high visual acuity to perform many daily activities required of them. Specifically, normal visual acuity is a pre-requisite for proper usage of most contemporary Graphic User Interfaces. The most common forms of visual acuity loss are myopia, hyperopia, and astigmatism. Contact lenses or glasses can easily correct these simple visual aberrations. There exist, however, more complex aberrations that cannot be easily remedied by such means. These "high-order" aberrations are modeled through what is known as the Point Spread Function (PSF) of the human eye. The PSF can be obtained indirectly through the wavefront aberration function of the human eye, currently accessible through wavefront analyzers. Thus, it is feasible that with the knowledge of the PSF, digital images could be altered according to a transformation opposite to the one they suffer in an aberrated eye. Consequently, when they are displayed to the user, he /she will perceive them undistorted. This paper presents an image processing approach, based on deconvolution of the PSF from the intended computer images that achieves this objective. The theoretical foundation of the approach is introduced along with simulation results using actual PSFs from subjects.

1. Introduction

Advances in the computer industry have made computers pervasive in our daily life. The common interface for humans to use computers is via visual information, presented on a digital display, such as cathode ray tubes (CRT) or liquid crystal displays (LCD) screens. Consequently, the ability to reasonably interpret the information presented in the Graphic User Interfaces (GUIs) directly impacts a human being's ability to use computers effectively.

Interpretation of GUI visual information occurs at many levels in the human visual and cognitive systems. If there are errors present at any point in the systems, the user will be unable to effectively interact with the computer. This paper addresses errors present in the refractive part of the visual system, that is, any error that can be described by the eye's Point Spread Function.

Several common types of refractive visual errors or aberrations occur in human eyes. If these errors are present, the result is a loss of visual acuity, which is necessary for basic interaction with the PC [6]. The most common types of these aberrations are myopia, hyperopia, and astigmatism. Lenses have been used to overcome these types of visual limitations, (e.g., defocus), in one way or another since the XIII Century. Further developments in ophthalmology during the last century have resulted in improved methods of correction, such as contact lenses, and recently, Laser-Assisted In Situ Keratomileusis (LASIK) surgery. Although very effective, these forms of correction however only apply to these common aberrations. They are not suited to deal with high-order aberrations such as keratoconus [8].

Previous attempts at correcting these high order aberrations [7, 11] are bulky and require very expensive custom equipment. Although these methods are effective, their complexity and high cost render them impractical for everyday use [2]. More recently, an all-digital solution has been proposed [2]. In contrast with the optical correction of visual limitations, this approach is based on modifying the image at its source, i.e., applying image processing modifications on the image to be displayed on-screen

before it is shown to the user, based on the knowledge of his/her own wavefront aberration function.

Because this method is based on knowing the mathematical representation of the refractive error, it should apply equally well to both low-order (myopia, hyperopia, etc.) as well as high order aberrations. The aim of the pre-compensation proposed in this paper is essentially the same; "modify the intended display image in a way that is opposite to the effect of the wavefront aberration of the eye. Once this is achieved, the result is displayed to the viewer so that the wavefront aberration in the viewer's eye will "cancel" the pre-compensation, resulting in the projection of an undistorted version of the intended image on the retina" [2]. However, the means towards achieving the pre-compensation proposed here overcomes some of the limitations of the previous attempt at an all-digital, software solution.

Since the proposed method of pre-compensation is entirely digital, i.e. the method is implemented completely in software, any Personal Computer (PC) capable of running a 32-bit operating system with an SVGA graphics card can be used to deliver the pre-compensation. The only other component necessary is the PSF of the user, which can be obtained through wavefront analysis of the user's eye. This measurement is performed through wavefront analyzers, currently becoming more and more common in ophthalmologist's and optometrist's offices [5]. With these components, the method implemented in software and the PSF of the user, the interface will then be customized to the aberration present in the user's visual system, allowing him/her to view the display screen as if there were no aberration present.

The paper is organized as follows. We begin by summarizing the current research, showing examples and analysis of the limitations encountered. The inverse processing using the PSF is then described, followed by the description of an improved version of the Weiner filter and post- processing for contrast enhancement of the pre-compensated images. Simulation results follow, along with the Discussion, and Conclusion.

2. Current Research

The human eye is an imaging system and behaves in a manner similar to any type of imaging system composed of lenses [10], forming an image at their effective focal length. Any object, when being viewed by the eye, can be thought of as a two-dimensional array of points of varying intensity [12]. Thus, for an eye free of aberrations, each point in the object is represented as a point on the retina. Ideally then, when a human views a computer screen, each pixel can be thought of as a point-source of light, and the corresponding image of that pixel is projected onto the retina [2].

If the eye is unable to project a point source of light onto the retina as a corresponding point, the result is a broad Point Spread Function (PSF), which describes the light distribution on the retina caused by each point of light in the object. This introduces a blurring effect in the retinal image.

The PSF of the human eye can be found indirectly through what is known as the wavefront aberration function, which represents the deviation of the light wavefront from a purely spherical pattern as it passes the pupil on its way to the retina [9]. Equations 1, 2, and 3 describe the method by which to obtain the PSF, *PSF(x,y)*, from the Wavefront aberration function, *W(x,y)* [2, 4, 9, 10, 12],

$$P(x,y) = A(x,y)e^{-j\cdot 2\cdot\pi\cdot n\cdot W(x,y)/\lambda} \tag{1}$$

$$OTF(fx,fy) = P(x,y) \otimes P^*(-x,-y) \tag{2}$$

$$PSF(x,y) = F^{-1}\{OTF(fx,fy)\} \tag{3}$$

where *P(x,y)* is the pupil function, *P*(-x,-y)* is the complex conjugate of the pupil function, *A(x,y)* is the amplitude attenuation across the pupil plane, usually set equal to one, *OTF(fx,fy)* is the Optical Transfer function, n is the index of refraction, λ is the wavelength of light in a vacuum, and $F^{-1}\{\ \}$ denotes the inverse Fourier transform [9].

The relationship between the object, (i.e. the digital display device) and the image projected on the retina is described by convolution [9, 10], which is summarized by equation 4.

$$I(x,y) = O(x,y) \otimes PSF(x,y) \tag{4}$$

where I(x,y) is the retinal image, O(x,y) is the object and $\otimes$ denotes convolution.

Under these same assumptions, the object can be reconstructed from the degraded retinal image through convolution with the inverse PSF:

$$O(x,y) = I(x,y) \otimes PSF^{-1}(x,y) \tag{5}$$

where $PSF^{-1}(x,y)$ is the inverse of the PSF.

This inverse process is referred to as "deconvolution". If the deconvolution is applied to the undistorted image, a pre-compensated image will be created. When viewed through the PSF, this pre-compensated image will be projected onto the retina, free of distortion [2].

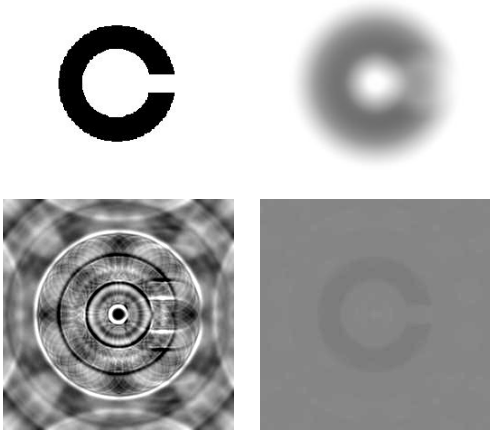

(a)(b)
(c)(d)

Figure 1. Sequence of convolution and pre-compensation

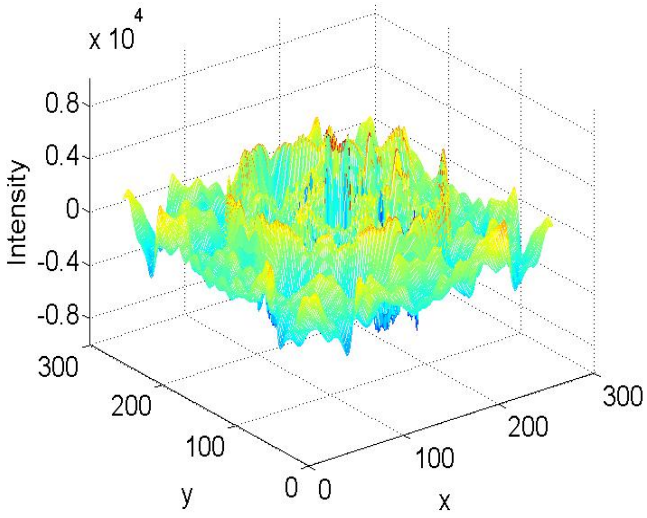

Figure 2. Direct result of pre-compensation

This process is illustrated in frequency by

$$PC(fx,fy)=\left[[OTF(fx,fy)]^{-1}\cdot\frac{|OTF(fx,fy)|^2}{|OTF(fx,fy)|^2+K}\right]O(fx,fy) \quad (6)$$

where *PC(fx,fy)* is the Fourier transform of the pre-compensated image, and K is a constant-valued parameter used to regulate the deconvolution.

Figure 1 shows the entire sequence of convolution and pre-compensation using the methods described above, assuming that the object displayed to the user is in fact a digital image that can be presented on a digital display. The PSF is assumed to be a spherical aberration, or defocus. Figure 1-a is the object, which in this case is a letter 'C', figure 1-b is the object as a user with a low-order spherical refractive error would view it, figure 1-c is the result of the pre-compensation using equation 6 and taking the inverse Fourier transform of *PC(fx,fy)*, and figure 1-d is what the user would see when viewing the pre-compensated image.

As is shown in figure 1, the processing of an intended digital representation of the letter 'C' using the deconvolutional method of pre-compensation results in a restoration of the letter assuming a defocus PSF. There are however two unwanted side –effects of the processing: the apparent loss of contrast (figure 1-d) and the introduction of low-frequency artifacts (which are present even in figure 1-c).

2.1 Contrast loss

Figure 1 illustrates the idea of pre-compensating an image and also illustrates the loss of contrast due to the intensity scaling that must be applied to the pre-compensated image in order to display it on the computer monitor. Thus, performance of this approach is ultimately influenced by the ability of the computer monitor to accurately reproduce the required intensities. Given that all digital displays can only reproduce positive intensities in the range of [0 255], a suitable adaptation to the method must be implemented.

The direct result of using equation 6 produces a pre-compensated image that contains both negative and positive values, shown in figure 2. The pre-compensated image ranges from -6,857.1 to 8,333.7. The solution explored in [1] is to shift and scale the intensity values to lie in a range of [0 1], or for display on a digital screen, [0 255]. This can be accomplished using equation 7:

$$PCS=\frac{\left(PC-\min(PC)\right)}{\max\left(PC-\min(PC)\right)}\cdot 255 \quad (7)$$

where *PC* is the pre-compensated image generated using equation 6, min and max are the absolute minimum and maximum of the pre-compensated image, respectively, and *PCS* is the scaled pre-compensated image.

2.2 Consequences of Intensity Scaling

A direct result of intensity scaling is to reduce the level of contrast in the final image that is projected onto the retina of the user, figure 1-d. It was found that the intensity scaling does not affect the frequency components in the pre-compensated image because the intensity scaling is a linear transformation. It affects only the DC and amplitudes of the frequency components by multiplication with a constant. Convolution with the inverse PSF itself does not affect the DC component of the image. This convolution

only applies to changing the relative amplitudes of the non-zero frequency terms. Thus, if the same contrast loss is introduced in advance into the original image of the letter 'C' (by changing the DC and the amplitude linearly), it will yield the same result as if the intensity scaling is applied to the pre-compensated image. As such, the sequence of convolution and pre-compensation, yielding displayable values of intensity, is illustrated in figure 3.

2.3 Low-frequency artifacts

Additionally, this form of pre-compensation introduces unwanted low frequency artifacts that, although not noticeable in figure 1-d, will hinder any attempts at post-processing the pre-compensated image to enhance its contrast. Those artifacts will be disproportionately amplified by the contrast enhancement. If for example, adaptive histogram equalization is applied to the pre-compensated image, as in [2], the final image viewed by the user with a defocus aberration, for instance, will be something like figure 4-b projected onto his/her retina.

The introduction of these low-frequency artifacts is attributed to the inverse processing. Using straight deconvolution to achieve the pre-compensation is essentially dividing the Fourier transform of the Object by the Fourier transform of the PSF. For values of the PSF near zero this will produce disproportionately high amplitude noise at the frequencies where these zeros occur.

The remedy is to use the Weiner filter of equation 6, which provides for a parameter K that can be adjusted to minimize the impact of these rogue frequencies [1, 3]. This constant value K works well for high frequencies, but does not adequately provide control of lower frequencies. Figure 5 shows the spectrum of the pre-compensated image using a constant value.

There are 4 frequencies which are disproportionately larger than the DC component, located in the center. These points coincide with the zeros of the PSF, which can be seen in the spectrum of the PSF, shown in Figure 6.

Therefore, a constant K will not produce the ideal result: having a pre-compensated image that is free of the unnecessary low-frequency artifacts while preserving the necessary frequencies that will allow the object to be perceived without blur by the user.

3. Method

The Weiner filter is typically used in the presence of Gaussian noise. The parameter K should ideally represent the spectrum of the signal to noise ratio. But often, the noise is not known, and its spectrum cannot be calculated.

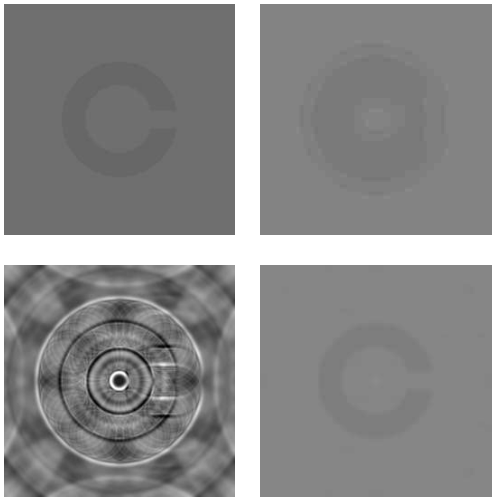

(a)(b)
(c)(d)

Figure 3. True sequence of convolution and pre-compensation

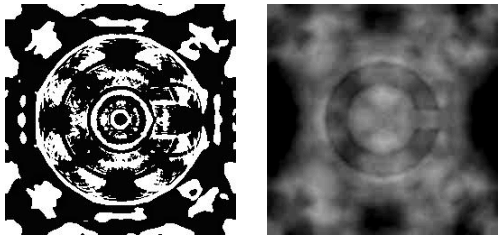

(a)(b)

Figure 4. Adaptive histogram pre-compensated image (a) and retinal projection (b)

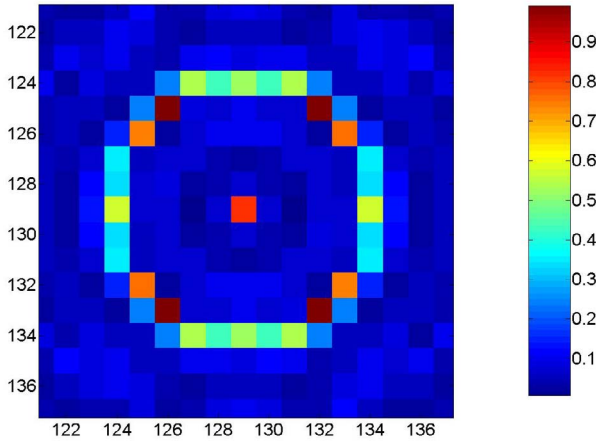

Figure 5. Spectrum of the pre-compensated image

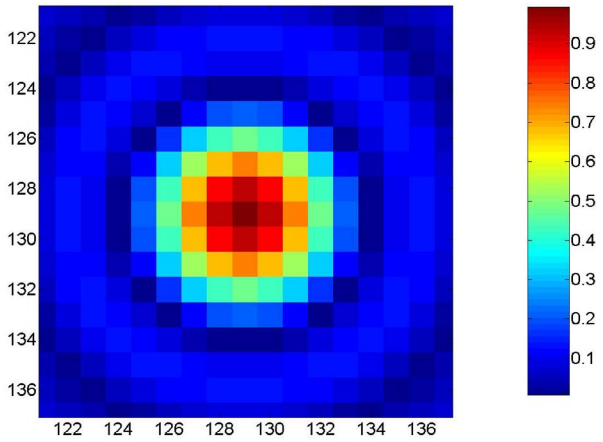

Figure 6. Spectrum of the PSF

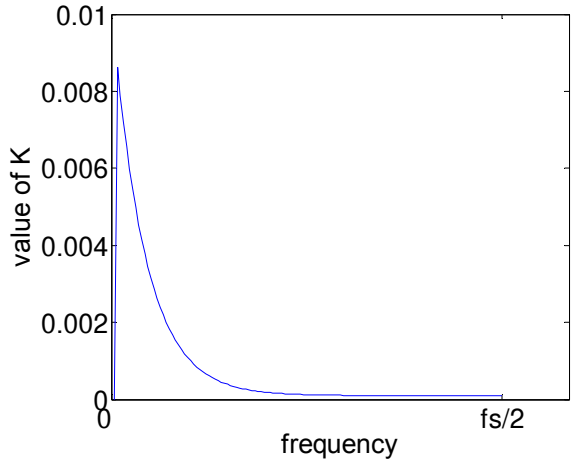

Figure 7. 1-D example of K varying with frequency *a*=9, *b*=0.0001, *α* = 12

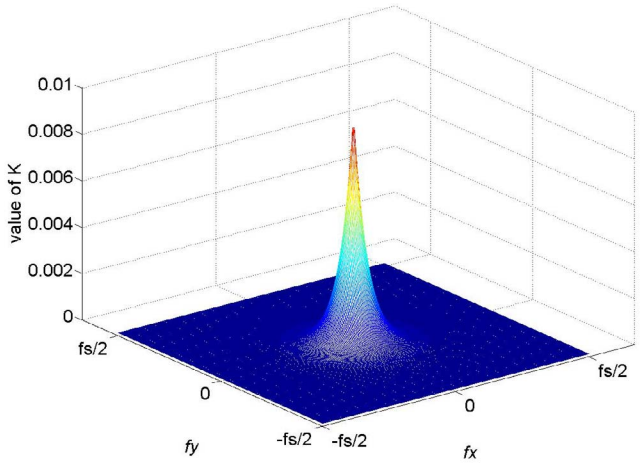

Figure 8. Variable K *a*=9, *b*=0.0001, *α* = 12

Thus, a constant value can be used in place of the spectrum of the signal to noise ratio [3], yielding acceptable results.

This is the approach taken in [1] and [2]. If instead, a variable value of K, based on frequency, is used, it is possible to reduce the introduction of noticeable low-frequency artifacts that are unavoidable with a constant K.

3.1. Enhanced Weiner Filter

As K approaches zero, the deconvolution using the Weiner filter (equation 6) converges to the ideal inverse filter [3]. Similarly, as the value of K increases, the effect of zeros in the PSF diminishes. The drawback of increasing the value of K is that the resulting inverse PSF is less accurate as the value of K increases.

In order to provide for a more accurate inverse PSF, while simultaneously reducing the appearance of low-frequency artifacts, a compromise between the values of K at high-frequencies and low-frequencies must be implemented.

In order to achieve this, a K that varies smoothly according to frequency is necessary:

$$K(f\theta, fR) = \begin{cases} a \cdot b \cdot e^{-\alpha R} + b & fR \neq 0 \\ 0 & fR = 0 \end{cases} \quad (8)$$

with

$$fR = \sqrt{fx^2 + fy^2} \quad (9)$$

and

$$f\theta = \tan^{-1}(fy/fx) \quad (10)$$

where $f\theta$ and fR represent the frequency in polar coordinates, assuming that the zero frequency is in the center of the spectrum, a is the span of K and b is the baseline value of K.

Figure 7 shows a one-dimensional representation of equation 8. The value of K at zero frequency is zero, allowing the deconvolution at zero frequency to be ideal. For frequencies other than zero, K is equal to a decaying exponential function that varies with frequency, ranging from 0.0009 for low frequencies, and approaching an asymptote at 0.0001. The steepness of the decaying exponential is controlled by the parameter α. Notice that the value of K remains fairly constant from fs/8 to fs/2. This preserves the high frequency deconvolution with a value of K=0.0001. For low frequencies however, the value begins to increase as the frequency decreases towards zero. This has the effect of 'toning down the low-frequencies in

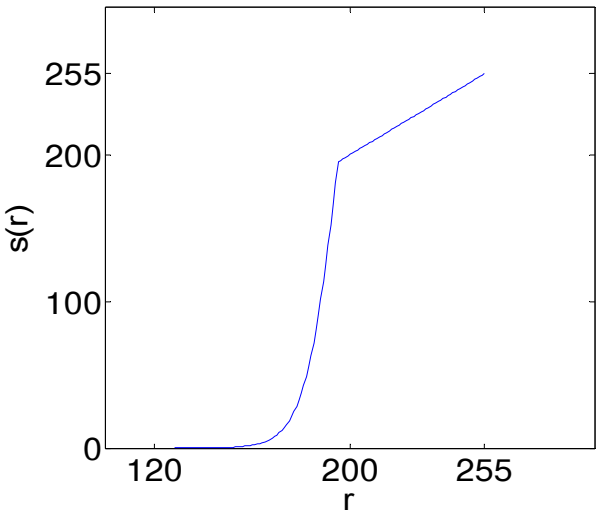

Figure 9. Gray level transformation of equation 9 with β=10, l=195, and u=128

relation to all of the other frequencies. Equation 8 is shown in figure 8.

3.2. Single-Sided Contrast Enhancement

While the use of a frequency varying K eliminates the low-frequency artifacts, the issue of the contrast loss still remains. A traditional histogram equalization method can be used, but it is too general. A better solution would be to incorporate knowledge of the original digital image and use that information to do post-processing contrast enhancement. This idea was implemented in the contrast enhancement proposed in [1]. The idea is to separate the letter from the background in the pre-compensated image.

Once this separation takes place, the background is then replaced by the background in the original image. Although this method provided some contrast enhancement, it introduced a 'halo' around the final retinal projection [1].

The fact that the shifting and scaling does not affect the non-zero frequencies can be used to aid the contrast enhancement. Ideally, the intensity of the background of the pre-compensated image should be somewhere near the intensity of the background in the original image. Thus, once the pre-compensated image is generated, it can be shifted and scaled in such a way that the mean is a gray level closer to the original background gray level. It is not advisable to replace exactly the background gray level of the original image because if the gray level is for instance white (as in figure 1-a) the remaining values of the pre-compensated image that lie above the mean would be shifted to values that are larger than 255, which cannot be displayed. Thus, the shifting and scaling for a pre-compensated image derived from figure 1-a for example,

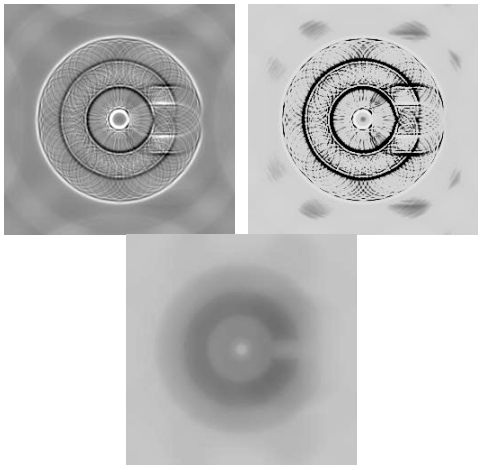

(a)(b)
(c)

Figure 10. (a) Enhanced Weiner Filter (b) Figure 10-a processed using single-sided contrast enhancement approach (c) Projected retinal image of figure 10-b

would place the mean level of the pre-compensated image near white.

Since the restoration of the focus is governed by non-zeros frequencies, the transients in the pre-compensated image should be preserved through the entire contrast enhancement process. Thus, a one sided, or single-sided method of contrast enhancement is necessary. This can be implemented as follows:

$$s(r)=\begin{cases} r & r>l \\ \dfrac{1-e^{-\beta\left(\frac{r-u}{l-u}-1\right)}}{1+e^{-\beta\left(\frac{r-u}{l-u}-1\right)}}\cdot l+l & r\le l \end{cases} \quad (11)$$

where s(r) is the transformation, r is the gray level, β is the parameter controlling the steepness of the transformation, l is the threshold level, and u is the minimum value of the pre-compensated image after it has been shifted and scaled to have a mean near the background gray level. In brief, this transformation essentially raises the background level of the pre-compensated image close to white. Figure 9 shows the grayscale transformation with β=10, l=195, and u=128.

Notice that for gray levels above l, the transformation is a one to one transference, but for gray levels that lie below l, the negative half of a bipolar sigmoid function is used. This allows for a smooth, controlled gray level transformation.

The values for β, l, and u will depend on the pre-compensated, scaled and shifted image. The value of l should be sufficiently below the mean of the pre-

compensated, scaled and shifted image so as to minimize the transformation of unwanted low-frequency noise.

4. Simulation Results

Figure 10 shows the pre-compensated images and projected retinal images when both the enhanced Weiner filter, and the single-sided contrast enhancement algorithms are applied to the original letter 'C'.

5. Discussion

Figure 10-a shows the reduction of the low-frequency artifacts that the normal Weiner filter introduces (visible, for example, in figure 3-c). This reduction is a pre-requisite for post-processing to increase the contrast of only areas that have transients present. Once this image is generated, it is then shifted and scaled to a mean value near white. For the images in figure 10, the shifting and scaling produced a pre-compensated image with the mean gray level at 222, the maximum at 255, and the minimum at 195. This image was then processed using the single-sided contrast enhancement algorithm with β=10, l=195, and u=221 (Figure 10-b). Figure 10-c is a simulation of the resulting projected retinal image that a user having a spherical aberration (defocus) would perceive when viewing figure 10-b.

6. Conclusion

The simulations shown above have illustrated the potential of the image pre-compensation approach proposed to revert the degradation on the perception of images presented on digital displays. Improvements on the Weiner filter, as well as a gray level transformation resulted in a higher contrast when the pre-compensated image is viewed through the aberration than achieved by previous methods.

The next stage of our work will use the methods developed to generate the pre-compensation for participants with targeted visual impairments, particularly those of high-order. This will allow verification of the general applicability of the algorithms.

We foresee that this pre-compensation approach will be applicable to users with severe refractive errors whose individual wavefront aberration functions are known.

7. Acknowledgements

This work was sponsored by NSF grants IIS-0308155, HRD-0317692 and CNS-0426125. Miguel Alonso Jr. is a recipient of the National Science Foundation Graduate Research Fellowship.

8. References

[1] M. Alonso Jr. and A. Barreto, "An Improved Method of Pre-Deblurring Digital Images Towards the Pre-Compensation of Refractive Errors," *WSEAS Transactions on Computers*, vol. 3, pp. 487-492, 2004.

[2] M. Alonso Jr., A. Barreto, J. G. Cremades, and J. A. Jacko, "Image pre-compensation to facilitate computer access for users with refractive errors," *Accepted for publication in the Behaviour and Information Technology Journal (BIT)*, 2005.

[3] R. C. Gonzales and R. E. Wood, *Digital Image Processing*. New Jersey: Prentice Hall, 2002.

[4] J. W. Goodman, *Introduction to Fourier Optics*. New York: McGraw-Hill Book Company, 1968.

[5] J. Hjortdal, "Book Review: Wavefront and Emerging Refractive Technology," *ACTA Ophthalmologica Scandanavia*, vol. 81, pp. 681, 2003.

[6] J. A. Jacko, A. B. Barreto, G. J. Marmet, J. Y. Chu, H. S. Bautsch, I. U. Scott, and R. H. Rosa, "Low Vision: The Role of Visual Acuity in the Efficiency of Cursor Movement," Proceedings of the Fourth International ACM Conference on Assistive Technologies (ASSETS '00), Arlington, VA, 2000, pp.1-7.

[7] J. Liang, D. R. Williams, and D. T. Miller, "Supernormal vision and high-resolution retinal imaging through adaptive optics," *Journal of the Optical Society of America*, vol. 14, pp. 2884-2892, 1997.

[8] J. N. Parker and P. M. Parker, *The official patient's sourcebook on Keratoconus: A revised and updated directory for the internet age*. San Diego: Icon Health Publications, 2002.

[9] T. O. Salmon, "Corneal Contribution to the Wavefront Aberration of the Eye," in *School of Optometry*. Bloomington: Indiana University, 1999.

[10] L. N. Thibos, "Formation and Sampling of the Retinal Image," in *Seeing: Handbook of Perception and Cognition*, K. K. D. Valois, Ed., 2 ed. San Diego: Academic Press, 2000, pp. 1-54.

[11] L. N. Thibos, X. Qi, and D. T. Miller, "Vision through a liquid crystal spatial light modulator," Proceedings of the 2nd International Workshop on Adaptive Optics for Industry and Medicine, Singapore, 1999, pp.57-62.

[12] R. G. Wilson, *Fourier Series and Optical Transform Techniques in Contemporary Optics: An Introduction*. New York: John Wiley and Sons, Inc., 1995.